Advanced Composite Materials

ISSN: 0924-3046 (Print) 1568-5519 (Online) Journal homepage: http://www.tandfonline.com/loi/tacm20

Preparation and properties of La-doped barium ferrite/poly (3-methylthiophene) composites

Helin Hua, Jinmei Liu, Yu Xie, Zhanggao Le, Yuanfu Yu, Rong Zhong, Yuancheng Qin, Yan Huang, Guisheng Zeng, Yunhua Gao & Yun Ling

To cite this article: Helin Hua, Jinmei Liu, Yu Xie, Zhanggao Le, Yuanfu Yu, Rong Zhong, Yuancheng Qin, Yan Huang, Guisheng Zeng, Yunhua Gao & Yun Ling (2015) Preparation and properties of La-doped barium ferrite/poly (3-methylthiophene) composites, Advanced Composite Materials, 24:1, 17-26, DOI: 10.1080/09243046.2013.871176

To link to this article: http://dx.doi.org/10.1080/09243046.2013.871176

Published online: 08 Jan 2014.

Advanced Composite Materials, 2015
Vol. 24, No. 1, 17–26, http://dx.doi.org/10.1080/09243046.2013.871176

Preparation and properties of La-doped barium ferrite/poly (3-methylthiophene) composites

Helin Hua[a], Jinmei Liu[a], Yu Xie[a]*, Zhanggao Le[b]*, Yuanfu Yu[a], Rong Zhong[a], Yuancheng Qin[a], Yan Huang[a], Guisheng Zeng[a], Yunhua Gao[c] and Yun Ling[a]

[a]*College of Environment and Chemical Engineering, Nanchang Hangkong University, Nanchang 330063, P.R. China;* [b]*Department of Applied Chemistry, East China Institute of Technology, Fuzhou 344000, P.R. China;* [c]*Key Laboratory of Photochemical Conversion and Optoelectronic Materials, Technical Institute of Physics and Chemistry, Chinese Academy of Sciences, Beijing 100190, P.R. China*

(*Received 4 November 2012; accepted 23 July 2013*)

La-doped barium ferrite/poly(3-methylthiophene)(LB/P3MTH) composites have been successfully synthesized by in suit chemical polymerization with ferrite chloride ($FeCl_3$) as an initiator. The composites structure is investigated by X-ray diffraction analysis (XRD) and Fourier transform infrared spectroscopy, and the morphology of samples is observed by transmission electron microscopy (TEM). Magnetic properties of the composites are tested by vibrating sample magnetometer. XRD analysis shows that La^{3+} has got into the lattice of Ba-ferrite and replaces the Ba^{2+} and that the best La^{3+} amount of La-doped Ba-ferrite is not more than 0.08. La-doped Ba-ferrite particles are coated with poly (3-methylthiophene). TEM image reveals that La-doped Ba-ferrite particles have spherical morphology and are agglomerated due to the coated polymer. P3MTH covers the ferrite surface and has crystallite boundaries, which influences the composites' physical and chemical properties.

Keywords: barium ferrite; rare earth; 3-Methylthiophene; composites; magnetic properties

1. Introduction

Recently, ferrite nanoparticles have attracted great attention because they can absorb radiation energy from microwave generated from an electric source. Much attention has been paid to ferrite materials due to their useful electromagnetic properties in a large number of applications.[1] It is well known that the resistivity of the ferrites is very high. The magnetic loss of these materials results from their ferrimagnetisms. The resonance reflects loss of moving magnetic domains and spins relaxation in the high frequency alternating electromagnetic fields.[2,3] The M-type hexagonal ferrites are special kinds of absorbing materials due to their dielectric and magnetic losses in the microwave frequency band. The materials have been studied extensively as high frequency devices because of their high resistivity, low eddy current losses, high-Curie temperature, mechanical hardness, and chemical stability.[4–7]

Conducting polymers have attracted significant attention in recent decades because of their potential applications in various fields such as electromagnetic interference

*Corresponding authors. Email: yuxie@nchu.edu.cn [Y. Xie]; zhgle@ecit.edu.cn [Z. Le]

shielding, rechargeable battery, chemical sensor, corrosion devices, and microwave absorption.[8–12] Among these conducting polymers-based composites, the PANI/ferrite composites have a complementary synergy behavior between PANI and ferrite nanoparticles.[13–16] Polythiophenes (PTh) polymers have been widely used in environmentally and thermally stable conjugated polymer materials such as electrical recording materials, nonlinear optical devices, polymer light-emitting diodes and displays, electrochromic or smart windows, antistatic coatings, sensors, batteries, electromagnetic shielding and imaging materials, artificial noses and muscles, solar cells and transistors, nanoswitches, polymer electronic interconnects, and DNA protection [17–26] because of their excellent environmental and thermal stability. Several interesting research papers have focused on PTh–metal oxide composites to obtain materials with advanced mechanical and chemical properties, which can be used in many application fields.[27–30]

In the present work, an investigation was made to obtain La-doped barium ferrite/poly (3-methylthiophene)(LB/P3MTH) via the sol–gel method and *in situ* chemical polymerization revealed the influence of the La-doping amount on the obtained samples and the effect of the P3MTH polymerization on the physical and chemical properties of LB.

2. Experimental

2.1. Materials

3-methylthiophene was purchased from Sigma. Lanthanum nitrate ($La(NO_3)_3{\cdot}6H_2O$), barium nitrate ($Ba(NO_3)_2$), ferric nitrate ($Fe(NO_3)_3{\cdot}9H_2O$), ferric chloride ($FeCl_3$), citric acid, and polyethylene glycol were all analytical reagent and used as received. Other reagent was also analytical grade.

2.2. Preparation of LB

The starting materials were analytically grade pure of $Ba(NO_3)_2$, $La(NO_3)_3{\cdot}6H_2O$, $Fe(NO_3)_3{\cdot}9H_2O$, and citric acid. $BaLa_xFe_{12-x}O_{19}$($x = 0.00$, 0.04, 0.08, 0.12) particles were prepared through the sol–gel route. Stoichiometric amount of these materials was mixed in deionized water and then dissolved in citric acid thoroughly. When the pH value of the solution was adjusted to weak acidic with ammonia water, the color was changed from brown-yellow. The system stopped being stirred at 80 °C until the wet gel was formed. And then, the gel was dried at 90 °C under vacuum. The xerogels were calcined at 950 °C for 2 h after grinding (Table 1).

2.3. Preparation of LB/P3MTH

Composites were prepared by *in situ* chemical polymerization in aqueous solution. A proper amount of ferrite particles and trichloromethane was dissolved in aqueous

Table 1. The stoichiometric amount of every material used to prepare $BaLa_xFe_{12-x}O_{19}$ particles.

	$Ba(NO_3)_2$/g	$La(NO_3)_3{\cdot}6H_2O$/g	$Fe(NO_3)_3{\cdot}9H_2O$/g	$C_8H_8O_7{\cdot}H_2O$/g
$x = 0.00$	1.96146	0	36.36170	20.48710
$x = 0.04$	1.96063	0.13029	36.23719	20.49000
$x = 0.08$	1.96026	0.25993	36.11923	20.49010
$x = 0.12$	1.96012	0.38864	25.99710	20.48866

solution. The system stopped being stirred 2–3 min until dark green solution. Then, the solution was added to P3MTH and LB and stirred in a water bath at 90 °C for 8 h after dried. The LB/P3MTH was formed.

2.4. Characterization

The composites structure was investigated by X-ray diffraction analysis (XRD, Rigaku model D/max-2500 system at 40 kV and 100 mA of cuka). The morphology of samples was observed by transmission electron microscopy (TEM, a JEM-3010 operating at 300 kV). The Fourier transform infrared spectroscopy (FTIR) spectra of the composites samples in KBr pallets were obtained using Model NlcolETiS10 Fourier transform spectrometer (Thermo Scientific Co., USA) with a 2 cm^{-1} resolution in range of 400–4000 cm^{-1}. The magnetic properties were investigated by vibrating sample magnetometer model 9600.

3. Results and discussion

3.1. XRD patterns of $BaLa_xFe_{12-x}O_{19}$

Figure 1 shows the XRD of the $BaFe_{11.92}La_{(0.08-x)}Nd_xO_{19}$ ($x = 0.00$, 0.04, 0.08, 0.12) of the temperatures at 950 °C. Figure 1 shows the characteristic peaks of ferrite and the hexaferrite structure including the peaks at $2\theta = 30.3°$, 32.2°, 34.1°, 37.1°, 40.3°, 55.0°, 56.3°, and 63.1°, which is the characteristic peak is similar to the standard ICDD PDF. According to Figure 3, it is observed that La^{3+} replaces Fe^{3+}.

In addition, when the La-doped amount is not more than 0.08, the samples phase was pure Ba-ferrite. However, when the La-doped amount was more than 0.08, there emerged the peaks of $LaFeO_3$ and Fe_2O_3, which shows that the La^{3+} has got into the lattice of Ba-ferrite and replaces the Ba^{2+}. La^{3+} has the different valence with Ba^{2+}, which causes lattice internal vacancy. The result shows that the optimum La amount of La-doped Ba-ferrite is not more than 0.08.

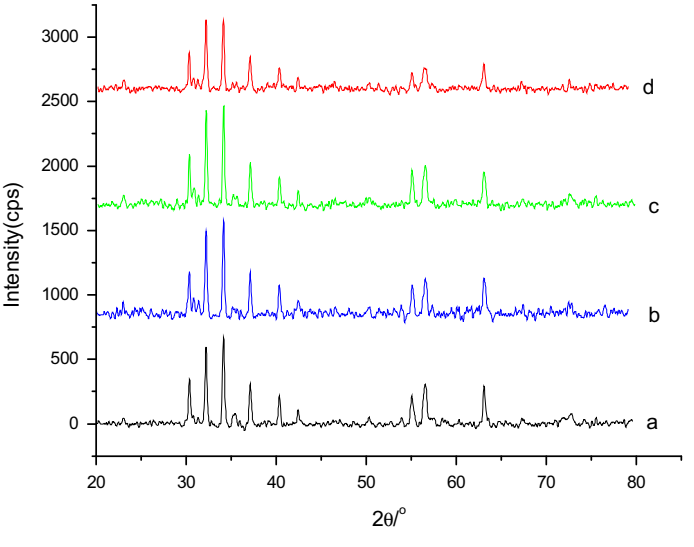

Figure 1. XRD patterns of $BaLa_XFe_{12-x}O_{19}$ at 950 °C for 2 h (a) $x = 0.00$, (b) $x = 0.04$, (c) $x = 0.08$, and (d) $x = 0.12$.

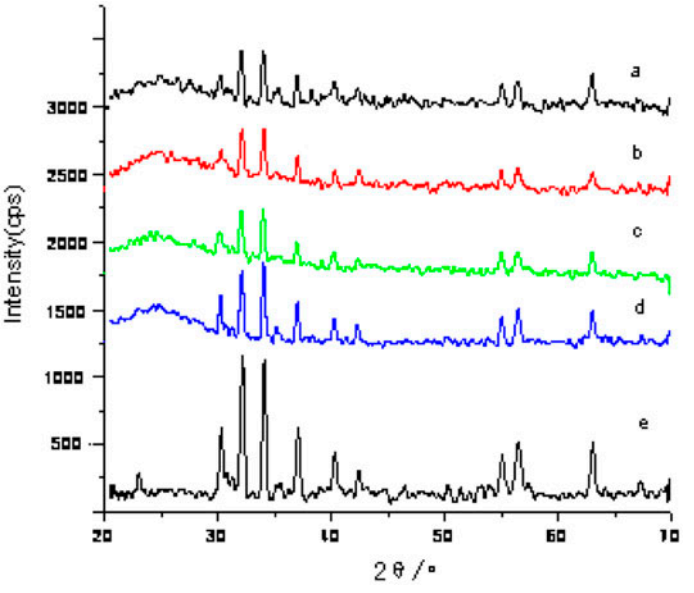

Figure 2. XRD patterns of $BaLa_xFe_{12-x}O_{19}$/P3MTH (a) $x = 0.00$, (b) $x = 0.04$, (c) $x = 0.08$, (d) $x = 0.12$, and (e) $BaLa_{0.08}Fe_{11.92}O_{19}$.

3.2. *XRD patterns of $BaLa_xFe_{12-x}O_{19}$/P3MTH*

Figure 2 shows that a, b, c, and d are X-ray diffraction patterns of $BaLa_XFe_{12-x}O_{19}$ at 950 °C, and e is the hexaferrite of patterns of $BaLa_{0.08}Fe_{11.92}O_{19}$. Figure 2(a)–(d) shows broad diffraction peak centered in the range of $2\theta = 21–27°$. This proves that the

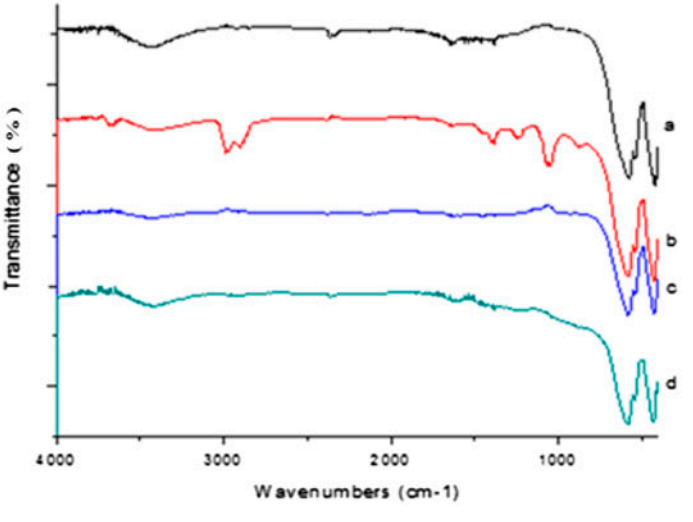

Figure 3. FTIR spectra of $BaLa_XFe_{12-x}O_{19}$ at 950 °C for 2 h (a) $x = 0.00$, (b) $x = 0.04$, (c) $x = 0.08$, and (d) $x = 0.12$.

$BaLa_xFe_{12-x}O_{19}$/P3MTH is amorphous structure. As shown in Figure 2, the diffraction peak position and diffraction intensity of $BaLa_{0.08}Fe_{11.92}O_{19}$ composites are reduced to the as-prepared $BaLa_xFe_{12-x}O_{19}$/P3MTH, which reveals that Ba-ferrite particles are best coated with P3MTH.

3.3. FTIR spectra analysis

Figure 3 shows the FTIR spectrograms of the $BaLa_XFe_{12-x}O_{19}$ of composites. In Figure 3, there are obvious characteristic stretching vibration absorption peak located in the lower frequency of $BaLa_XFe_{12-x}O_{19}$ at the range of 600–580 cm^{-1} is assigned to tetrahedral of hexaferrite structure. However, obvious characteristic stretching vibration absorption peak located in the lower frequency of $BaLa_XFe_{12-x}O_{19}$ at the range of 440–400 cm^{-1} is assigned to octahedral of hexaferrite structure.

Figure 4 shows the FTIR spectrograms of $BaLa_xFe_{12-x}O_{19}$/P3MTH composites. In this picture, the peaks at approximately 2986 cm^{-1} are attributed to the characteristic stretching vibrations of saturated C–H of methyl. The peaks at approximately 1383 cm^{-1} are attributed to symmetry deformation vibration of CH_3-of 3-methylthiophene monomer. The peaks at approximately 910 cm^{-1} are attributed to antisymmetric and symmetric stretching vibration of C–S. The peaks at approximately 818 cm^{-1} are attributed to out-of-plane vibrations of C–H, which C–H substituted for 2,3,5-3-methylthiophene. It proves that 3-methylthiophene has happened by the polymerization reaction. The peaks at approximately 3434 cm^{-1} are attributed to the characteristic stretching vibrations of aqueous. The four characteristic peaks above have appeared shift. The reason may be that $BaFe_{12}O_{19}$ are coated by 3-methylthiophene molecular chains, and the chemical bonding reaction between them decreases the electron density on the polymer molecular chains, which affects the atomic vibration frequency and reduces the force constant between atoms.

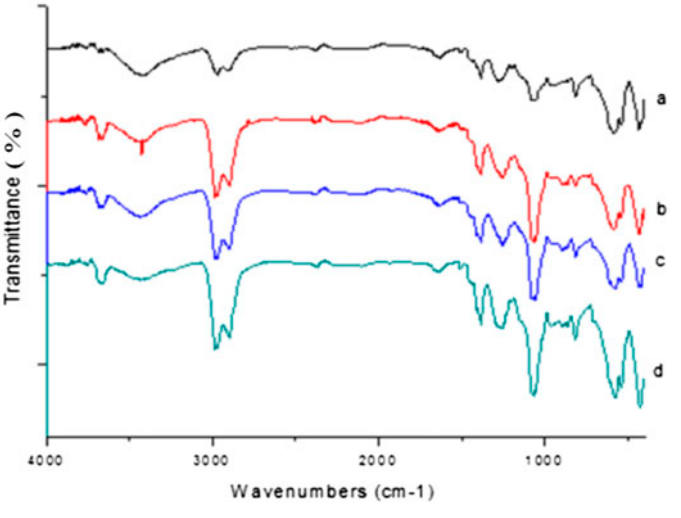

Figure 4. FTIR spectra of $BaLa_xFe_{12-x}O_{19}$/P3MTH (a) $x = 0.00$, (b) $x = 0.04$, (c) $x = 0.08$, and (d) $x = 0.12$.

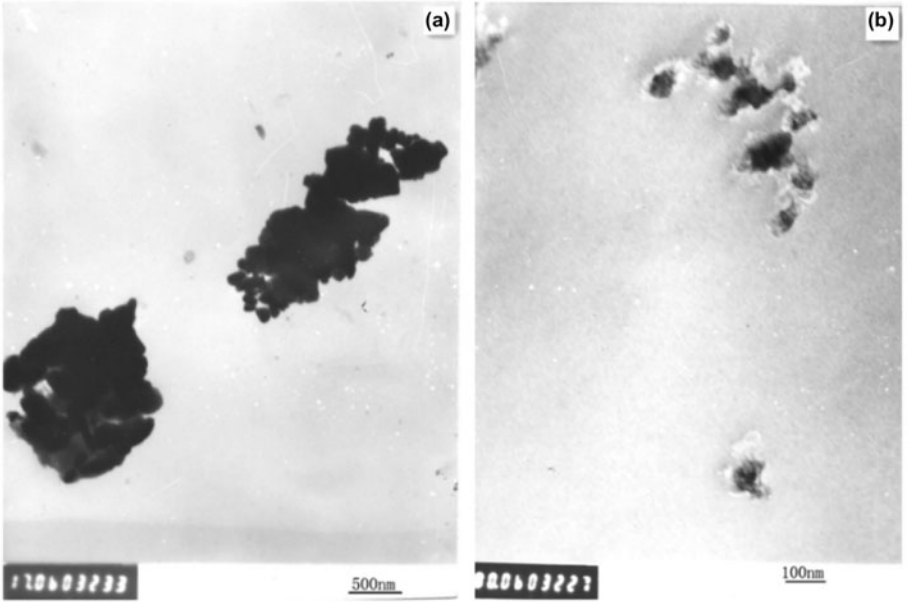

Figure 5. (a) TEM images of $BaLa_xFe_{12-x}O_{19}$, (b) TEM images of $BaLa_xFe_{12-x}O_{19}$/P3MTH.

3.4. *Transmission electron microscopy*

The morphology of LB/P3MTH composites and LB is shown in Figure 5(a) and (b).TEM images reveal that the ferrites particles are embedded in PMTH-3 matrix forming the core–shell structure. The size distribution diagram is presented in this picture. As shown in Figure 5(a), the structures of PMTH-3 coated LB-ferrite are

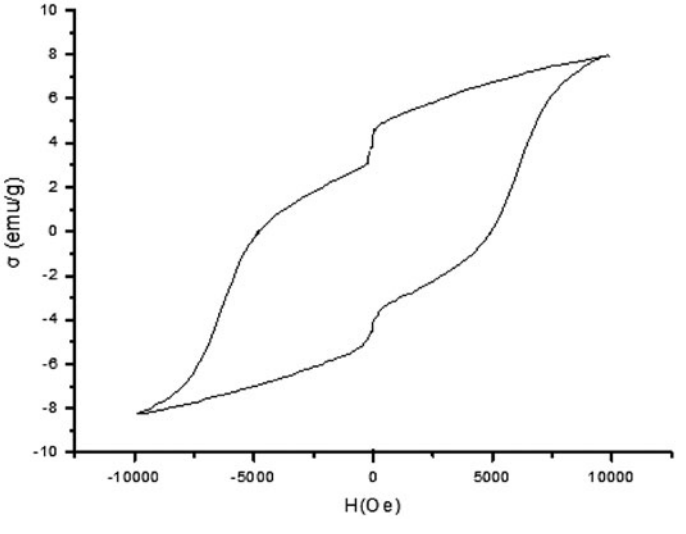

Figure 6. Hysteresis loops for $BaFe_{12}O_{19}$ at 950 °C.

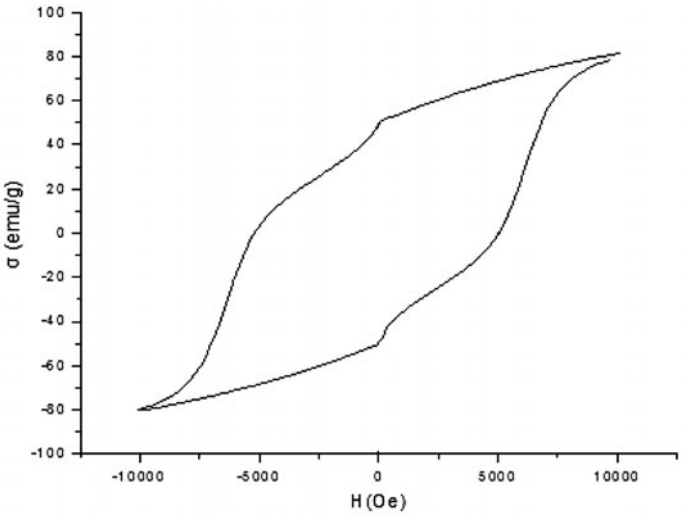

Figure 7. Hysteresis loops for $BaLa_{0.08}Fe_{11.92}O_{19}$ at 950 °C.

crowded. TEM image reveals that BL-ferrite particles are observed to have spherical morphology and are agglomerated due to the coated polymer.

3.5. *Magnetic properties analysis*

Figures 6–8 show the magnetization curves of (a) $BaFe_{11.92}La_{(0.08-x)}Nd_xO_{19}$, (b) $BaLa_{0.08}Fe_{11.92}O_{19}$, and (c) $BaLa_{0.08}Fe_{11.92}O_{19}$/P3MTH composites. The magnetization (M) curves are as a function of applied magnetic field (H). The magnetic properties, the saturation magnetization (Ms), the remanent magnetization (Mr), and the coercivity (Hc) were determined.

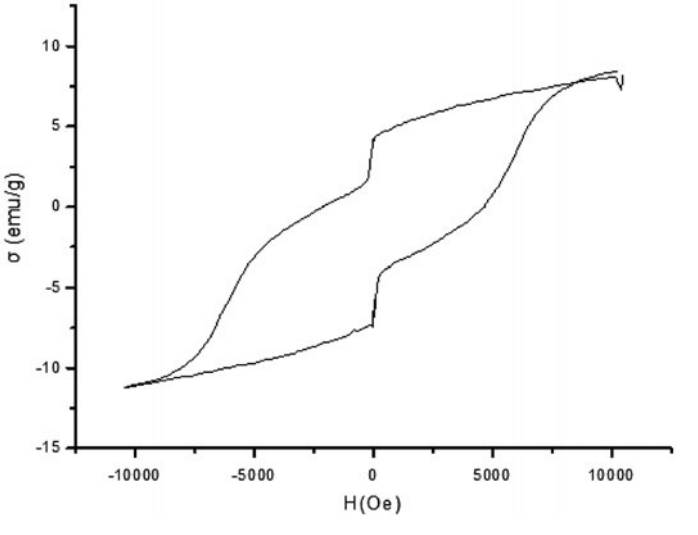

Figure 8. Hysteresis loops for $BaLa_{0.08}Fe_{11.92}O_{19}$/PMTH-3 at 950 °C.

Table 2. The $BaFe_{11.92}La_{(0.08-x)}Nd_xO_{19}$ magnetic parameters at 900 °C.

Composites	Coercivity (Hc/Oe)	Saturation magnetization (Ms/emu·g^{-1})	Remanent magnetization (Mr/emu·g^{-1})
$BaFe_{12}O_{19}$	4850	7.9	3.3
$BaLa_{0.08}Fe_{11.92}O_{19}$	5160	80.0	49.5
$BaLa_{0.08}Fe_{11.92}O_{19}$/ PMTH-3	3380	9.2	5.7

As shown in Table 2, the Ms of $BaFe_{12}O_{19}$ composites is 7.9 emu·g^{-1} and the value informs the ferromagnetic nature. The Ms of $BaLa_{0.08}Fe_{11.92}O_{19}$ composites is 80.0 emu·g^{-1}. The Ms of $BaLa_{0.08}Fe_{11.92}O_{19}$/P3MTH composites is 9.2 emu·g^{-1}. It can be observed that the Ms of $BaLa_{0.08}Fe_{11.92}O_{19}$ increases due to the doped rare earth of La. However, the Ms of $BaLa_{0.08}Fe_{11.92}O_{19}$/P3MTH decreases due to embedded in non-magnetic polymer matrix.[31–34] It is well known that Ms is related to the volume fraction of magnetic ferrite particles (φ) and the saturation moment of single particles (m_s).[35]

In the present study, the composites have lower Ms, Mr, and Hc (Table 1) values. The reason for lower Ms value is that there exists non-magnetic PMTH-3 in the composites. It is well known that polycrystalline ferrites have an irregular structure, geometric and crystallographic nature, such as pores cracks, surface defects. In the polymerization process, P3MTH covers the ferrite surface and crystallite boundaries, which leads to a decrease in coercivity. In addition, there may be the surface spinning of magnetic moments at ferrite nanoparticles/support interface,[36] which result in a decrease in magnetic surface anisotropy of ferrite particles. So, there is the coercivity of the $BaLa_{0.08}Fe_{11.92}O_{19}$/P3MTH decreased compared to that of $BaLa_{0.08}Fe_{11.92}O_{19}$.

4. Conclusions

In this study, rare earth-doped Ba-ferrites nanoparticles were synthesized via the sol–gel method. The electronic properties are successfully synthesized in the core–shell form by *in situ* chemical polymerization of P3MTH in the presence of $BaLa_{0.08}Fe_{11.92}O_{19}$ particles. XRD analysis shows that La^{3+} has got into the lattice of Ba-ferrite and replaces the Ba^{2+}, and the best amount of La-doped Ba-ferrite is not more than 0.08. La-doped Ba-ferrite particles are coated with P3MTH. TEM image reveals that La-doped Ba-ferrite particles have spherical morphology and are agglomerated due to the polymer coated. It was also demonstrated that the doped La^{3+} has led to the lattice distortion and has lowered the magnetic parameters of $BaFe_{12}O_{19}$. In addition, the $BaLa_{0.08}Fe_{11.92}O_{19}$ composites have the best crystallinity and the magnetic properties. We also come up with P3MTH which covers the ferrite surface and has crystallite boundaries, which influences the composites' physical and chemical properties.

Acknowledgments

This work was financially supported by the National Natural Science Foundation of China (No. 20904019, and 51273089), the Aviation Science Fund (No. 2011ZF56015, and 2013ZF56025), Natural Science Foundation of Jiangxi Province (No. 20132BAB203018), Key Laboratory of Photochemical Conversion and Optoelectronic Materials, TIPC, CSA (No. PCOM201228, and

PCOM201130), Jiangxi Province Education Department of Science and Technology Project (No. GJJ13491), Jiangxi Province Youth Scientists Cultivating Object Program (No. 20112BCB23017) and Key Laboratory of Jiangxi Province for Persistent Pollutants Control and Resources Recycle, Nanchang Hangkong University (No. ST201222007).

References

[1] Snelling EC, Shrivastava CM, Patni MJ, editors. Advances in ferrites. Vol. 1. New Delhi: Oxford & IBH; 1989. p. 579.
[2] Qiu J, Gu M, Shen H. Microwave absorption properties of Al- and Cr-substituted M-type barium hexaferrite. J. Magn. Magn. Mater. 2005;295:263–268.
[3] Sugimoto S, Haga K, Kagotani T, Inomata K. Microwave absorption properties of Ba M-type ferrite prepared by a modified coprecipitation method. J. Magn. Magn. Mater. 2005;290–291:1188–1191.
[4] Kumar PS, Shrotri JJ, Kulkarni SD, Deshpande CE, Date SK. Low temperature synthesis of $Ni_{0.8}Zn_{0.2}$ Fe_20_4 powder and its characterization. Mater. Lett. 1996;27:293–296.
[5] Mangalaraja RV, Ananthakumar S, Manohar P, Gnanam FD. Initial permeability studies of Ni–Zn ferrites prepared by flash combustion technique. Mater. Sci. Eng. A. 2003;355:320–324.
[6] Zahi S, Hashim M, Daud AR. Synthesis, magnetic properties and microstructure of Ni–Zn ferrite by sol-gel technique. J. Magn. Magn. Mater. 2007;308:177–182.
[7] Secrist DR, Turk HL. Electrical properties of high-density iron-deficient nickel-zinc ferrites. J. Am. Ceram. Soc. 1970;53:683–686.
[8] Mäkelä T, Pienimaa S, Taka T, Jussila S, Isotalo H. Thin polyaniline films in EMI shielding. Synth. Met. 1997;85:1335–1336.
[9] Kuwabata S, Masui S, Yoneyama H. Charge–discharge properties of composites of LiMn2O4 and polypyrrole as positive electrode materials for 4 V class of rechargeable Li batteries. Electrochim. Acta.1999;44:4593–4600.
[10] Kan JQ, Pan XH, Chen C. Polyaniline–uricase biosensor prepared with template process. Biosens. Bioelectron. 2004;19:1635–1640.
[11] Ahmad N, MacDiarmid AG. Inhibition of corrosion of steels with the exploitation of conducting polymers. Synth. Met. 1996;78:103–110.
[12] Rose TL, D'Antonio SD, Jillson MH, Kon AB, Suresh R, Wang F. A microwave shutter using conductive polymers. Synth. Met. 1997;85:1439–1440.
[13] Li LC, Jiang J, Xu F. Novel polyaniline-LiNi0.5La0.02Fe1.98O4 nanocomposites prepared via an *in situ* polymerization. Eur. Polym. J. 2006;42:2221–2227.
[14] Jiang J, Li LC, Xu F. Preparation, characterization and magnetic properties of PANI/La-substituted LiNi ferrite nanocomposites. Chin. J. Chem. 2006;24:1804–1809.
[15] Jiang J, Li LC, Xu F. Polyaniline–LiNi ferrite core–shell composite: preparation, characterization and properties. Mater. Sci. Eng. A. 2007;456:300–304.
[16] Xie Y, Hong XW, Wang XY, Zhao J, Gao YH, Ling Y, Yan SF, Shi L, Zhang K. Preparation and electromagnetic properties of La-doped barium-ferrite/polythiophene composites. Synth. Met. 2012;162:1643–1647.
[17] Zhang M, Müller AHE. Cylindrical polymer brushes. J. Polym. Sci., Part A: Polym. Chem. 2005;43:3461–3481.
[18] Skotheim TA, Elsenbaumer RL, Reynolds JR, editors. Handbook of conducting polymers. 2nd ed. New York: Marcel Dekker; 1998.
[19] Waugaman M, Sannigrahi B, McGeady P, Khan IM. Synthesis, characterization and biocompatibility studies of oligosiloxane modified polythiophenes. Eur. Polym. J. 2003;39:1405–1412.
[20] Karim M, Lee C, Lee MS. Synthesis and characterization of conducting polythiophene/carbon nanotubes composites. J. Polym. Sci., Part A: Polym. Chem. 2006;44:5283–5290.
[21] Perepichka IF, Perepichka DF, Meng H, Wudl F. Light-emitting polythiophenes. Adv. Mater. 2005;17:2281–2305.
[22] Perzon E, Wang X, Zhang F. Design, synthesis and properties of low band gap polyfluorenes for photovoltaic devices. Synth. Met. 2005;154:53–56.
[23] Ho H, Najari A, Leclerc M. Optical detection of DNA and proteins with cationic polythiophenes. Acc. Chem. Res. 2008;41:168–178.

[24] Mwaura JK, Zhao X, Jiang H. Spectral broadening in nanocrystalline TiO_2 solar cells based on Poly(phenylene ethynylene) and polythiophene sensitizers. Chem. Mater. 2006;18:6109–6111.
[25] Zou Y, Wu W, Sang G. Polythiophene derivative with phenothiazine−vinylene conjugated side chain: synthesis and its application in field-effect transistors. Macromolecules. 2007;40:7231–7237.
[26] Liu RC, Liu ZP. Polythiophene: synthesis in aqueous medium and controllable morphology. Chin. Sci. Bull. 2009;54:2028–2032.
[27] Ohlan A, Singh K, Chandra A, Dhawan SK. Conducting ferromagnetic copolymer of aniline and 3,4-ethylenedioxythiophene containing nanocrystalline barium ferrite particles. J. Appl. Polym. Sci. 2008;108:2218–2225.
[28] Zhang X, Lee JS, Lee GS, Cha DK, Kim MJ, Yang DJ, Manohar SK. Chemical synthesis of PEDOT nanotubes. Macromolecules. 2006;39:470–472.
[29] Janáky C, Visy C. Synthesis and characterization of poly(3-octylthiophene)/γ-$Fe2O_3$ nanocomposite – a promising combination of superparamagnetic–thermoelectric–conducting properties. Synth. Met. 2008;158:1009–1014.
[30] Uygun A, Yavuz AY, Sen S. Polythiophene/SiO2 nanocomposites prepared in the presence of surfactants and their application to glucose biosensing. Synth. Met. 2009;159:2022–2028.
[31] Xie Y, Hong XW, Gao YH, Li MJ, Liu JM, Wang J, Lu J. Synthesis and characterization of La/Nd-doped barium-ferrite/polypyrrole nanocomposites. Synth. Met. 2012;162:677–681.
[32] Cui L, Gu H, Xu H. Synthesis and characterization of superparamagnetic composite nanorings. Mater. Lett. 2006;60:2929–2932.
[33] Leslie-Pelecky DL, Rieke RD. Magnetic properties of nanostructured materials. Chem. Mater. 1996;8:1770–1783.
[34] Jacobo SE, Aphesteguy JC, Lopez Anton R, Schegoleva NN, Kurlyandskaya GV. Influence of the preparation procedure on the properties of polyaniline based magnetic composites. Eur. Polym. J. 2007;43:1333–1346.
[35] Sauzedde F, Elaissari A, Pichot C. Hydrophilic magnetic polymer latexes. 1. Adsorption of magnetic iron oxide nanoparticles onto various cationic latexes. Colloid Polym. Sci. 1999;277:846–855.
[36] Song Q, Zhang ZJ. Shape control and associated magnetic properties of spinel cobalt ferrite nanocrystals. J. Am. Chem. Soc. 2004;126:6164–6168.